Available online at www.eccomasproceedia.org
Eccomas Proceedia COMPDYN (2023) 741-758

ECCOMAS
Proceedia

COMPDYN 2023
9th ECCOMAS Thematic Conference on
Computational Methods in Structural Dynamics and Earthquake Engineering
M. Papadrakakis, M. Fragiadakis (eds.)
Athens, Greece, 12-14 June 2023

STRUCTURAL HEALTH MONITORING (SHM) OF POLYFYTOS BRIDGE AND EVALUATION OF ITS DYNAMIC PROPERTIES

Alexandros G. Chortis[1], Ioannis G. Ramandanis[1], Georgios I. Dadoulis[1], Lazaros N. Melidis[1], George C. Manos[1] and Konstantinos V. Katakalos[1]

[1] Lab. Strength of Materials and Structures, Aristotle University of Thessaloniki
chortisag@civil.auth.gr, giannisrama@gmail.com , dadoulis@civil.auth.gr, lnmelidis@civil.auth.gr, gcmanos@civil.auth.gr, kkatakal@civil.auth.gr

Abstract

Bridges are important structures contributing both to the economic development of a region and to the service of citizens. Polyfytos bridge is today the second longest bridge in Greece and among the most used bridges, as it is part of the national highway network that connects Western Macedonia with Southern Greece, bridging Polyfytos lake. It was designed by Ricardo Morandi and constructed in early 1970s. After 50 years of active operation, Polyfytos bridge showed some permanent deformations concentrated at the end of the cantilever beam. The present manuscript focuses on the identification of its dynamic properties utilizing in situ measurements and numerical approaches. The in situ measurements of the developed accelerations of the cantilever beam are evaluated and used to calibrate the numerical model and argue on its realism.

Keywords: In situ measurements, Numerical simulation, Modal analysis , Structural Health Monitoring.

ISSN:2623-3347
Peer-review under responsibility of the organizing committee of COMPDYN 2023.
doi: 10.7712/120123.10432.21194

1 INTRODUCTION

Bridges are vitally important structures for society. These structures must be inspected for structural soundness. It is therefore necessary to develop a simple method for the detection of structural damage. Structural health monitoring of a bridge allows the correct management decisions to be made, such as the maintenance or the demolition of it, [1] especially when it is subjected to excessive earthquake or wind loads, such bridges are the Rion-Antirion Bridge, the Tsing Ma Bridge, the Humber Bridge, etc. [2, 3, 4, 5]. From the past, many have been dealing with how to verify the structural integrity of a bridge. The Fryba et.al. [6] describe the load test and modal analysis of bridges than had been performed in the Czech and Slovak Republics since 1968. The Dohler et.al. [7] perform SHM on bridge s101 implementing statistical methods. Furthermore the Reynders et. al. [8] implement the SHM on two civil engineering structures, on a pre-stressed bridge which suffers from damage and on a building.

The basic principle of SHM is based on the comparison of the measured eigenmodes in the structure with those obtained from the theoretical background assuming that the structure had no faults. From the comparison of the theoretical eigenmodes with the in situ determined eigenmodes, significant conclusions can be derived for the structural health of the structure. As mentioned by Neves et. al. [9] there are two fault detection methods. The model-based method which is based on creating a finite element model of the investigated structure and identifying the fault against the existing condition. This method is indeed accurate but has a high computational burden as numerical simulations in complex structures are not always easy to construct and if not properly inspected can lead to errors. And the model-free method based on artificial intelligence i.e., algorithms that are created and trained to detect faults when the values measured on the field are out of range compared to the anticipated values. This method is employed by Neves et.al. [9]. The Zinno et.al. [10] addresses how the artificial intelligence can advance the (SHM). Many have now enhanced the methodology to pinpoint the location of the fault in the structure. The Hansen et.al [11] demonstrate a method of fault detection based on the eigenmodes of the construction. The Rosales et.al. [12] attempt to locate the crack and its properties in beam-like structures. The Rainieri et.al. [13] by means of an algorithm to accurately identify the modal parameters so that it can be used to monitor the tensile loads of the cable stays. The Mousavi et. al. [14] formulated a warning method if there is a fault in the structure based on the SHM method.

The Servia High Bridge after many years of operation showed certain defects. In this paper the implementation of the SHM method as well as the operational modal analysis (OMA) on this bridge is presented in order to verify the fault in the bridge structure. Parametric analysis of the modulus of elasticity is done for the purpose of the identification of the present state of condition.

The in situ measurement of the eigenmodes is done by placing accelerometers at specific positions. The measured acceleration values following the fast fourier transform provide the frequency spectrum diagram and from this the eigenfrequencies of the structure can be extracted using a variety of methodologies. The Peeters et.al. [15] also the Reynders et.al. [16] present several methods for detecting the eigenfrequencies of bridges. These methods are applied to Z24-Bridge, a three-span reinforced concrete bridge in Switzerland. The Magalhaes et.al. [17] explains in detail the evolution of SHM and gives an implementation example on an arch bridge; the author emphasizes that SHM is of high research interest and advancement; and finally presents three out-modal identification algorithms.

The peak-picking method is the most simple method of selection of the eigenfrequencies, i.e. the eigenfrequencies that exhibit a high degree of involvement in the frequency spectrum diagram are selected. Certainly there is uncertainty of selection and in this method Qu et.al. [18]

proposes a selection method when the peaks are near. For the correct implementation of SHM it is vitally important to select the correct eigenfrequencies. The Langone et.al. [19] filter the frequency contents with the aim of obtaining more accurate results for the (SHM) method is tested on the Z24 pre-stressed concrete bridge.

In order to measure the accelerations, some agitation of the structure is required. The passing vehicles can be used to agitate the structure says the Yang et.al.[20]. The Malekjafarian et.al. [21] demonstrate an algorithm for extraction of the eigenfrequencies from the passing vehicles. The Yang et.al. [22] used a single-axis device to determine the eigenfrequencies. For example the recording can be influenced by the velocity of a passing vehicle, it is also affected if the vehicle decelerates and also by the coarseness of the asphalt pavement, said researchers Yin et.al. [23].

2 A DESCRIPTION OF THE SERVIA BRIDGE

The Servia bridge is an Important construction project for the region of Western Macedonia as well as the whole of Greece. It was built in place of a smaller steel bridge that connected the two banks of the Aliakmonas River. With the formation of the artificial lake in 1973, the national highway connecting north-western Greece with central Greece had to be linked and in order to continue to exist. Therefore, there was an immediate necessity to construct a new bridge.

The bridge was constructed according to the symmetric balanced cantilever method and consists of 27 spans. The first 21 spans beginning from Servia as well as the final spans between piers 25-26 and 26-27. These 23 spans are built with 40 m long prefabricated beams, which are simply supported on platforms 1-21 and 25-27. At piers 22, 23 and 24 there are two-sided protrusions ('investigation zones') 30 metres in length on either side. Prefabricated Gerber beams 40 metres in length are supported on these protrusions. The piers were laid before the formation of the man-made reservoir, while the superstructure was formed and constructed after the creation of the reservoir. The bridge was originally designed to accommodate two traffic lanes, one for each driving direction. In its current state, however, it consists of one lane for a single direction equipped with traffic lights.

The existing condition of the bridge shows intense pathologies in certain positions. Fractures were observed at the ends of the piers at the joint with the Gerber beams. This phenomenon led to significant local bending and settling of the bridge deck which is evident to the naked eye. Due to the presence of these failures, the Technical Service of the Western-Macedonia regional unit has taken action to mitigate the bridge's stresses, such as reducing traffic speeds and bi-directional crossing.

3 METHODOLOGY

3.1 Recording method

The assessment of the dynamic properties of the bridge sections under review is carried out using the method of structural health monitoring. Namely, sensor "nodes" fitted with accelerometers are placed at the extremities of the deck for the purpose of recording the bridge's reactions in the vertical (z) plane, as illustrated in Figure 1.

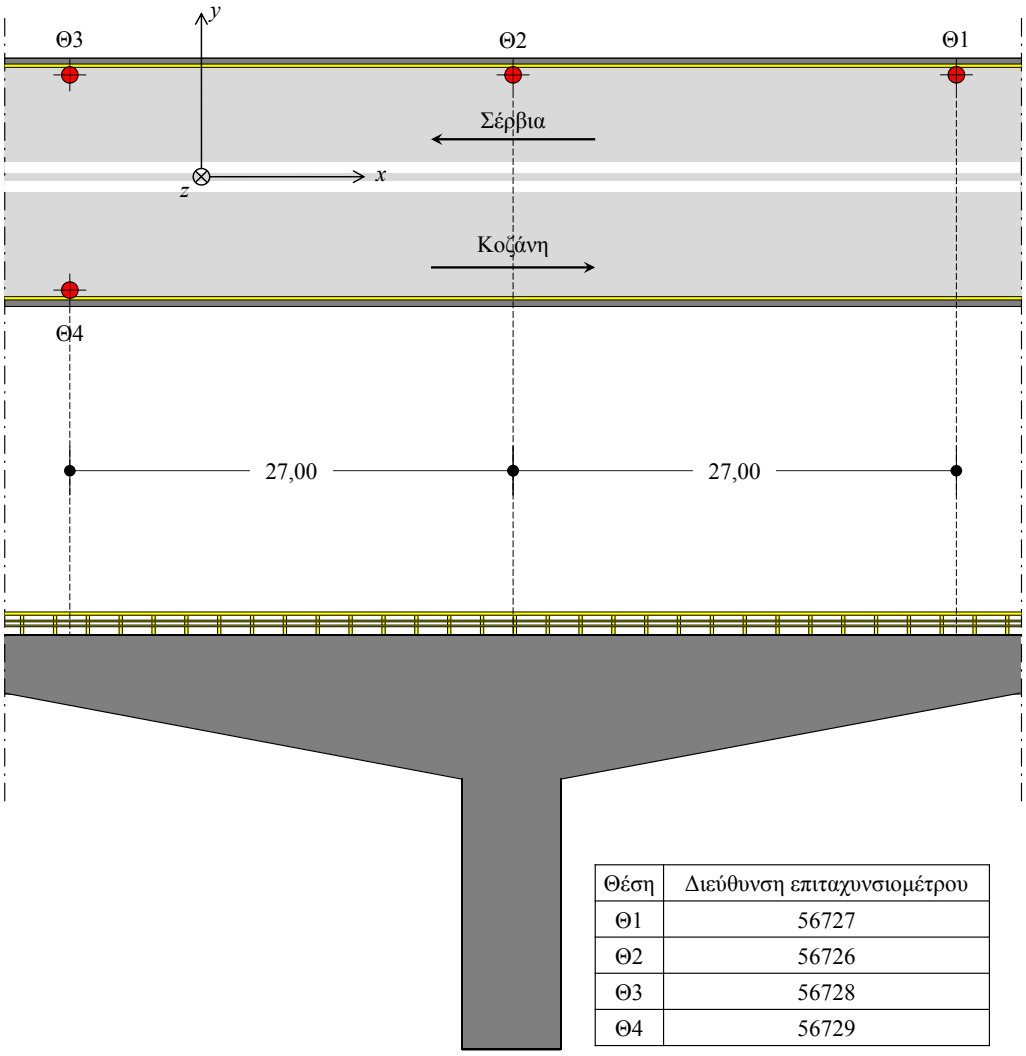

Θέση	Διεύθυνση επιταχυνσιομέτρου
Θ1	56727
Θ2	56726
Θ3	56728
Θ4	56729

Figure 1: Indicative arrangement of a bridge section.

The three successive sections of the bridge, M4, M5, M6, are organized in sequence, in which the piers are monolithically linked with protrusions on each side. The organization of each section is achieved by four sensor nodes, Θ1, Θ2, Θ3 and Θ4, three of which are placed along one edge of the deck, namely one at the level of the underlying pier (Θ2) and two on either side of that pier (Θ1, Θ3) at the distance of 27,00 m from the axis of the centre om mass of the pier. Lastly, node Θ4 is placed along the opposing edge of the deck symmetrical to node Θ3, in relation to the longitudinal axis of the bridge. The purpose of the installation is to record accelerations, which, after analysis of the data, leads to the extraction of dynamic characteristics of the bridge structure, such as eigenfrequencies and eigenmodes.

The sensor nodes used in the data logging are of the MicroStrain G-Link-200 type (Figure 2). Each node has an integrated accelerometer with a selectable acceleration recording range ranging from ±2 to ±40 g as well as an integrated temperature sensor [24]. The collection of accelerations from all nodes is achieved through a MicroStrain LORD WSDA-2000 [25] type "base unit", which is connected to a computer via USB and which handles all the wireless connections to the nodes, the automatic synchronization of the recordings and the collection of data from all nodes ("virtually") in real time. For the specified instrumentation, the base unit allows a "sampling frequency" of f_s = 64 Hz. In sections M4 and M5 one recording is obtained, while

in section M6 two recordings are obtained. Each recording is of approximately 10 min duration, under the effect of vehicle traffic in the standard practice of 'operational modal analysis' [26].

Figure 2: Sensor node used.

3.2 Method of extraction of measured eigenfrequencies

According to standard practices in OMA, the analysis of the data includes the transfer of the responses from the time domain to the frequency domain using the "Fast Fourier Transform" (FFT) and specifically using the Cooley-Tukey algorithm [27]. The eigenfrequencies are then extracted from the resulting plots using the peak-picking method. This method is a visual method, i.e. the values that have a significant value in the power spectra diagram are selected as the eigenfrequencies of the structure, i.e. those that are more heavily involved.

3.3 Finite elements model

Modal analysis of complex structures requires the creation of a numerical finite element simulation. The finite element method is based on the following equation.

$$M\ddot{u}\,(t) + C\dot{u}(t) + Ku(t) = p(t)$$

Where $\ddot{u}(t)$,$\dot{u}(t)$,$u(t)$ are vector time functions for each node within the finite element system, p(t) is the vector of external loads of each node while M, C, K are the mass, damping, stiffness matrices of the structure respectively.

At a programming level the procedure that is followed by the researcher in order to study a construction in order is as follows:

- The geometry of the construction is designed in a CAD program and a three-dimensional model is created.
- The model is divided into finite elements i.e., the mesh is created, and the resolution type is selected and any remaining data that is required is added. For instance, if it is selected for the model to be solved with statical stressing the data concerning the loads and the boundary conditions must be given. This procedure is done with software called pre-processors.
- When the parameters are ready for the resolution, they are entered in a program which will find the solution to the problem with numerical solutions as described previously. These types of programs are called solvers.
- When the solution is finalized, the results must be used in a program called a post processor in order for the engineer to see the results of the analysis.

3.4 Shell elements model

Thus, in this case as well, the complete structure of the bridge's 3 piers is designed. The geometry of the complete bridge was obtained from the initial design of Professor Morandi as well as from in situ measurements. Initially a numerical simulation was created using shell elements. Beam elements were used to simulate the pre-stressing and were placed within the shell elements. The location and number of prestressed tendons as well as the cross-section area of the tendons was derived from the initial design. The mass includes only the self weight of the structure. The prefabricated beams are supported on elastometallic bearings of an encased elastomer. The fixed N bearings prevent movement in both the vertical and the 2 horizontal planes. The NGe20 bearings limit movement in both the vertical and lateral planes, but in the longitudinal plane they allow the structure to move as much as 20 cm.

To simulate the bearings allowed to move in the longitudinal direction, a combination of Gap Elements and Body Constraints was used. In particular, at the end of each prefabricated beam, at one of its nodes, two (2) 2-Joint Links of Gap Element type were added, allowing movement on the longitudinal axis up to 20 cm. Each Gap Element only allows for movement in the longitudinal direction of the structure, while restricting the remaining movements. A Body Constraint is then assigned to the other end of each 2-Joint Link as well as to a node at the end of the protrusion, which binds all movements.

3.5 Solid elements model

A numerical simulation of solid finite elements is subsequently created. This contains only one platform this is done due to computational complexity. The purpose of this simulation is to place the mass as well as the geometry in the most precise manner possible. The information on geometry and prestressing is also obtained from the initial design and on-site surveys. The mass here also includes the self weight of the structure, while at the ends of the protrusions half of the mass of the Gerber beams is placed at the bearing positions of the bearings. The pre-stressing is also implemented here using beam finite elements. The structure soil interaction is not considered and in both numerical simulations the piers are supported with embedded conditions.

3.6 Analysis methodology

After creating two simulations, as described above, a parametric eigenmodal analysis was performed. Three cases of modulus of elasticity of the structure were defined in order to compare the observed condition with the condition derived from the numerical simulation. It is important to note that this paper investigates the eigenmodal concerning only the vertical component.

3.7 Materials

The numerical simulations take the values of the strengths of materials that were measured experimentally by taking castings from the current condition of the bridge also from the initial study of the bridge. These are presented in the following matrix.

Material	Characteristic tensile strength (MPa)
Concrete (B450)	32
Prestressed Steel	1062.91(breaking point)

Steel Rebar with ribs (StIIIa)	426.97 (yield point)

Table 1: Aggregate results of evaluation of mechanical properties of concrete and steel.

It is therefore concluded that the materials are in good condition and three scenarios of the modulus of elasticity of the bridge concrete are generated.

- E=17GPa
- E= 30 GPa
- E= 34 GPa

4 RESULTS

In the following pages, the results of the assessment of the dynamic characteristics of the structure from the data are summarized.

4.1 Operational modal analysis

The results of the accelerometers as well as the results of the Fourier transform are depicted. From these eigenfrequencies are selected with peak-picking method. These results concern the vertical aspect.

Section M4 - Direction z (vertical)

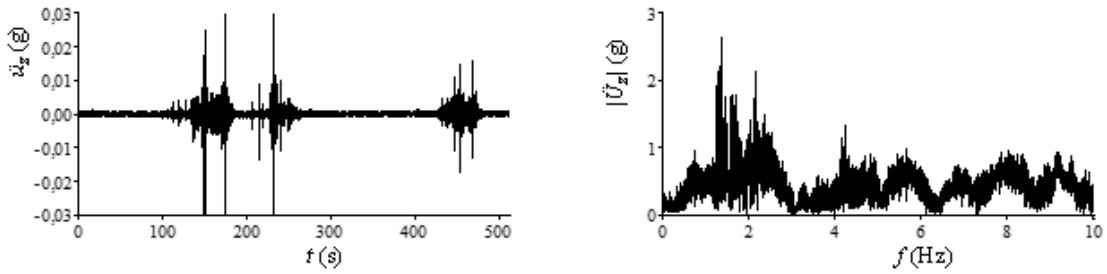

Figure 3: Acceleration response time histories for the integration of segment M4 in the vertical (z) aspect for Θ1 accelerometer also Fourier power spectra for the same record.

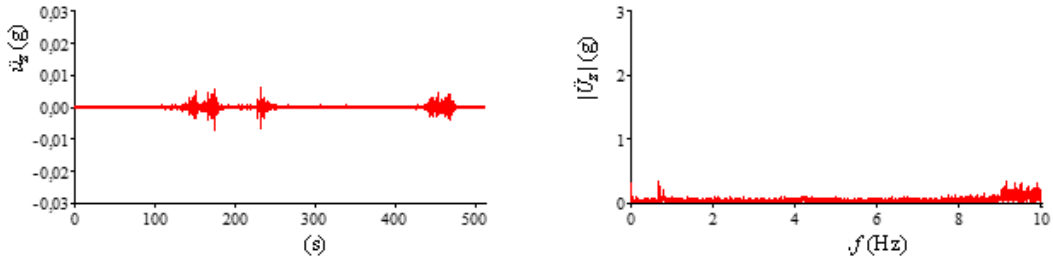

Figure 4: Acceleration response time histories for the integration of segment M4 in the vertical (z) aspect for Θ2 accelerometer also Fourier power spectra for the same record.

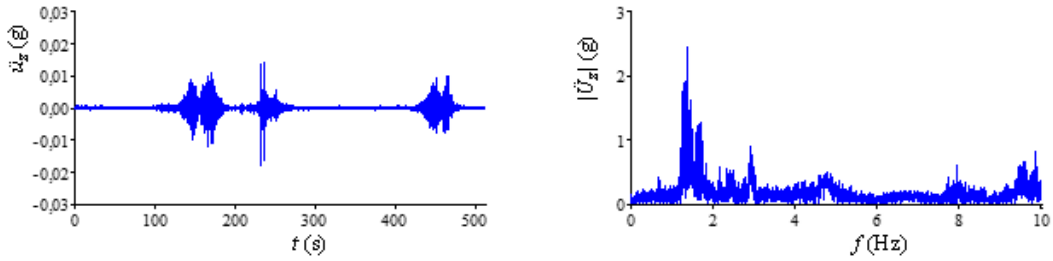

Figure 5: Acceleration response time histories for the integration of segment M4 in the vertical (z) aspect for Θ3 accelerometer also Fourier power spectra for the same record.

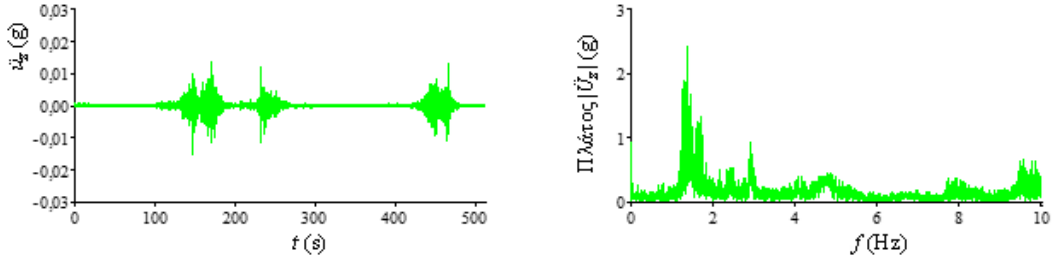

Figure 6: Acceleration response time histories for the integration of segment M4 in the vertical (z) aspect for Θ4 accelerometer also Fourier power spectra for the same record.

Section M5 - Direction z (vertical)

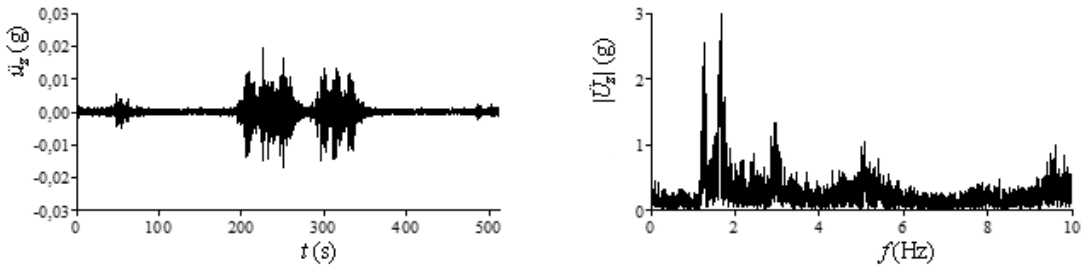

Figure 7: Acceleration response time histories for the integration of segment M5 in the vertical (z) aspect for Θ1 accelerometer also Fourier power spectra for the same record.

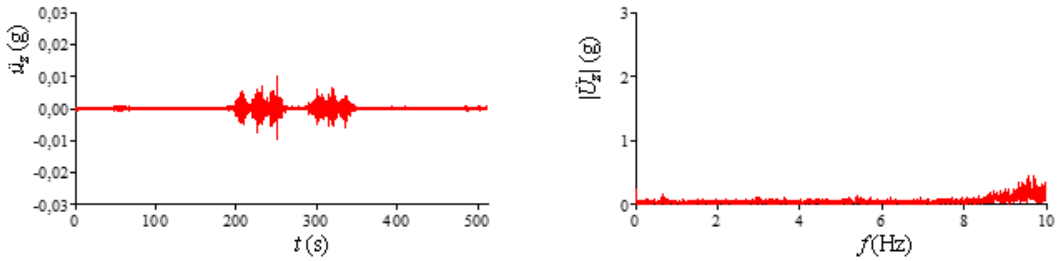

Figure 8: Acceleration response time histories for the integration of segment M5 in the vertical (z) aspect for Θ2 accelerometer also Fourier power spectra for the same record.

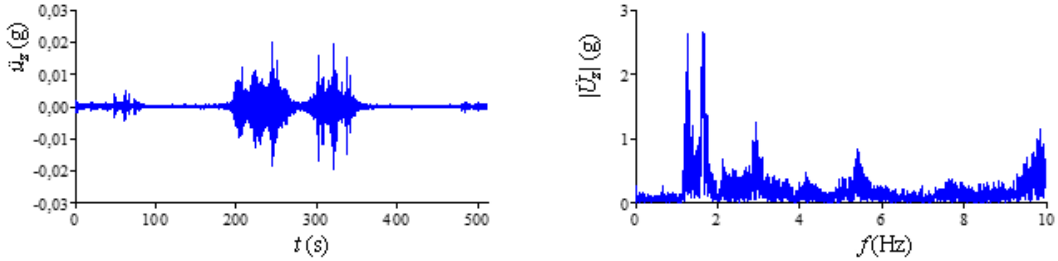

Figure 9: Acceleration response time histories for the integration of segment M5 in the vertical (z) aspect for Θ3 accelerometer also Fourier power spectra for the same record.

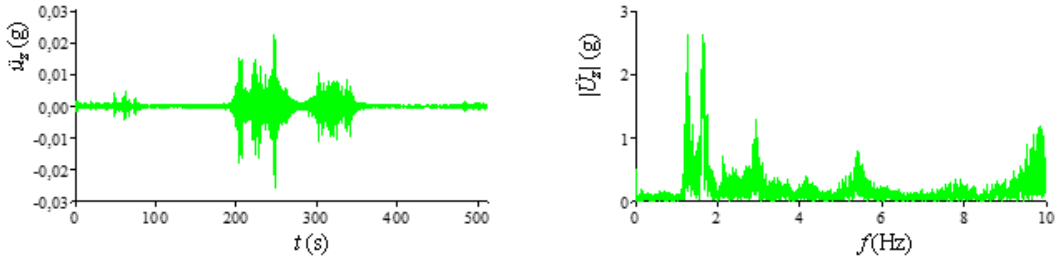

Figure 10: Acceleration response time histories for the integration of segment M5 in the vertical (z) aspect for Θ4 accelerometer also Fourier power spectra for the same record.

Section M6 (1st observation) - Direction z (vertical)

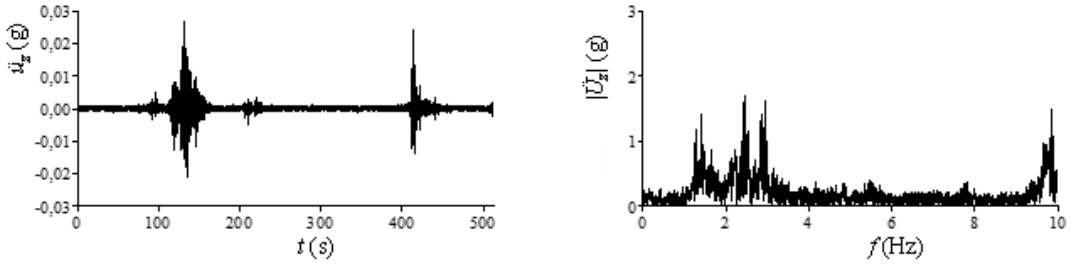

Figure 11: Acceleration response time histories for the integration of segment M6-1 in the vertical (z) aspect for Θ1 accelerometer also Fourier power spectra for the same record.

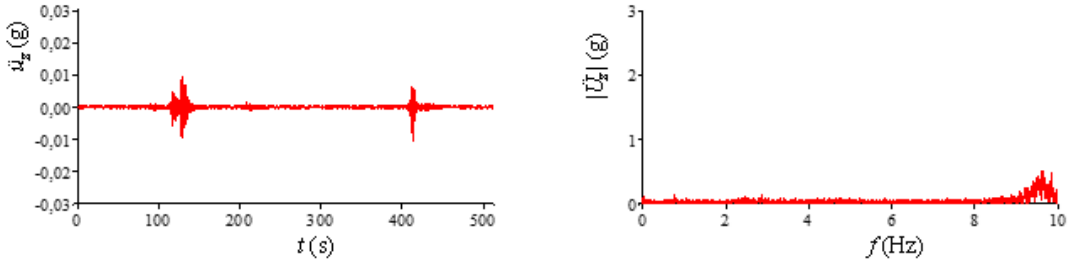

Figure 12: Acceleration response time histories for the integration of segment M6-1 in the vertical (z) aspect for Θ2 accelerometer also Fourier power spectra for the same record.

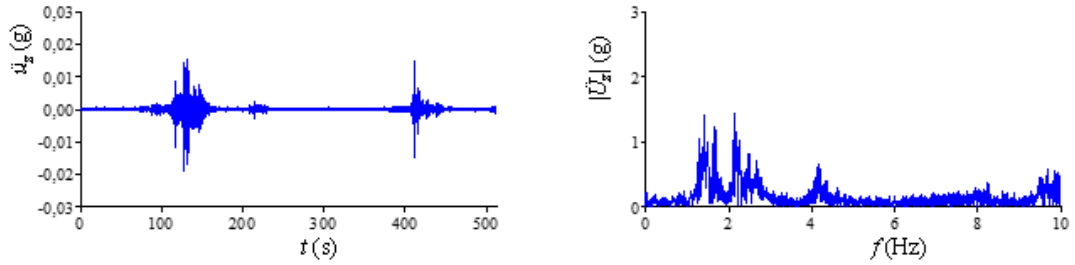

Figure 13: Acceleration response time histories for the integration of segment M6-1 in the vertical (z) aspect for Θ3 accelerometer also Fourier power spectra for the same record.

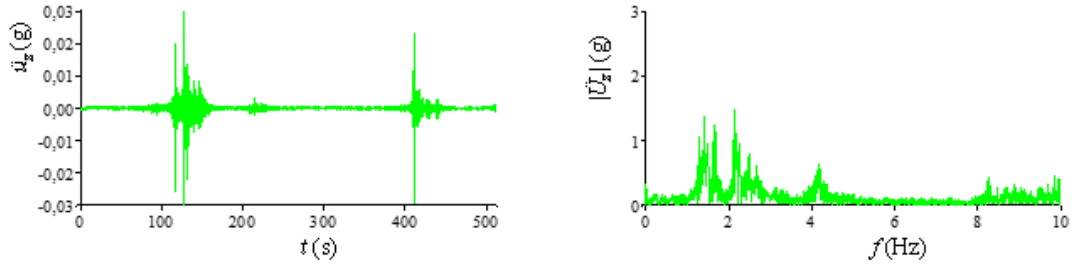

Figure 14: Acceleration response time histories for the integration of segment M6-1 in the vertical (z) aspect for Θ4 accelerometer also Fourier power spectra for the same record.

Section M6 (2nd observation) - Direction z (vertical)

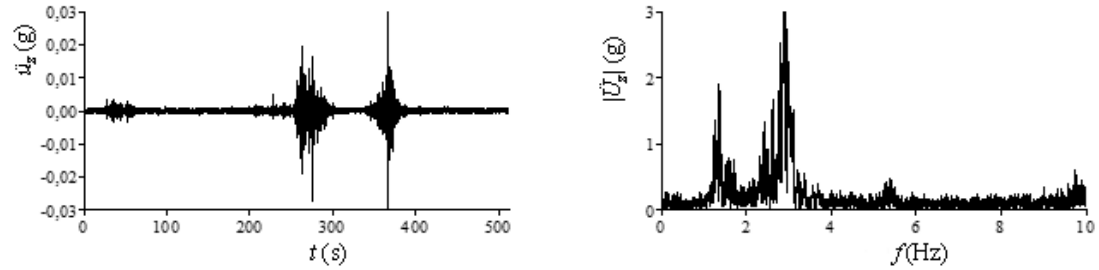

Figure 15: Acceleration response time histories for the integration of segment M6-2 in the vertical (z) aspect for Θ1 accelerometer also Fourier power spectra for the same record.

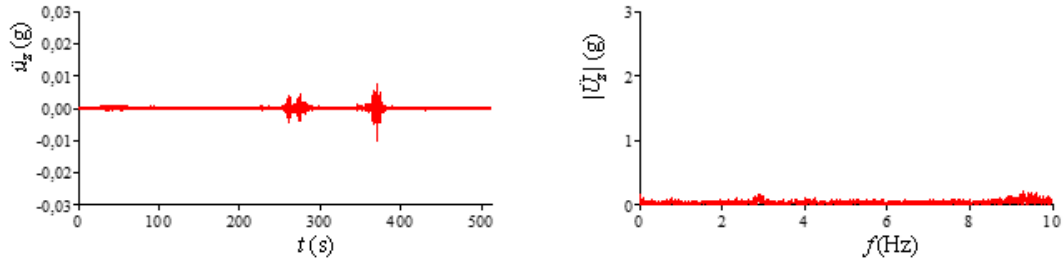

Figure 16: Acceleration response time histories for the integration of segment M6-2 in the vertical (z) aspect for Θ2 accelerometer also Fourier power spectra for the same record.

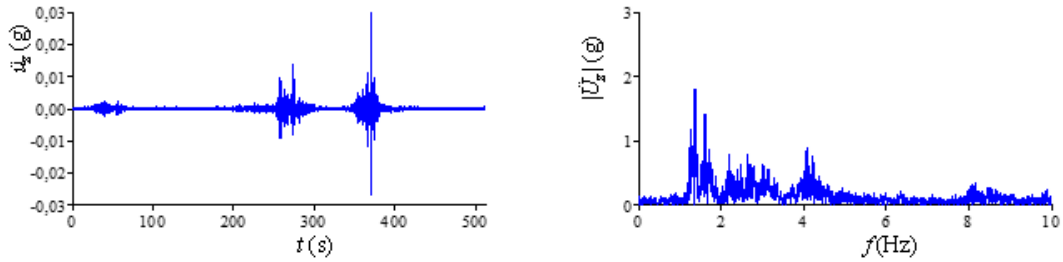

Figure 17: Acceleration response time histories for the integration of segment M6-2 in the vertical (z) aspect for Θ3 accelerometer also Fourier power spectra for the same record.

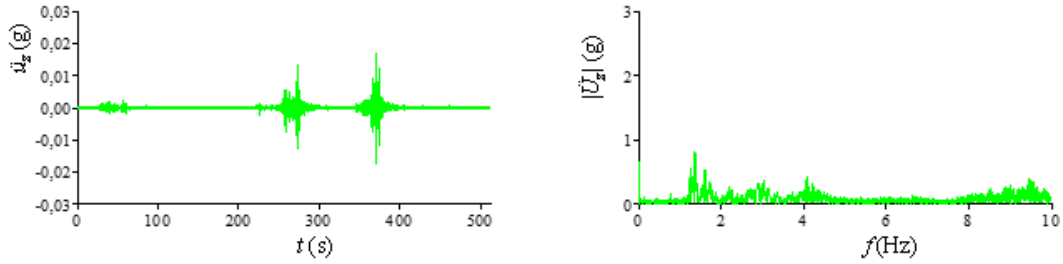

Figure 18: Acceleration response time histories for the integration of segment M6-2 in the vertical (z) aspect for Θ4 accelerometer also Fourier power spectra for the same record.

The frequency content of the responses in the vertical (z) aspect has different characteristics for each segment. The response of segment M4 shows rich frequency content in a range between 1,25-1,8 Hz, while the response of segment M5 shows frequency content in the same range, but dominated by two peaks, at 1,27 Hz and 1,67 Hz. Finally, the M6 section shows frequency content in the same frequency range, with the presence of peaks at 1,27 Hz and 1,67 Hz being less prominent. Also, the response of the M6 segment shows two additional peaks at approximately 2-2.5 Hz and 4 Hz. However, safe conclusions for this specific behavior can only be concluded by extracting eigenmodes and comparing them with the results of a dynamic analysis of the simulated structure. The peak-picking method is applied and the eigenfrequencies are selected.

	mode	M4	M5	M6-1	M6-2
Θ1	1	1.34	1.29	1.4	1.38
	2	2.14	1.7	2.47	2.857
	3	-	-	2.9	-
Θ3	1	1.34	1.28	1.4	1.36
	2	-	1.65	1.66	1.613
	3	-	-	2.13	-
Θ4	1	1.34	1.287	1.4	1.36
	2	-	1.625	1.66	1.613
	3	-	-	2.13	-

Table 2:Eigenfrequencies after peak-picking method for vertical direction.

4.2 Shell elements model

After modal analysis was done 15 eigenmodes were found for each of the tree cases of the young modulus. The following images show the most important eigenmodes for the case that young modulus equal to 34GPa. Below are depicted first and third mode because they had high mass participation factor. The eigenmodes that could be identified in vertical direction are 10 and 12.

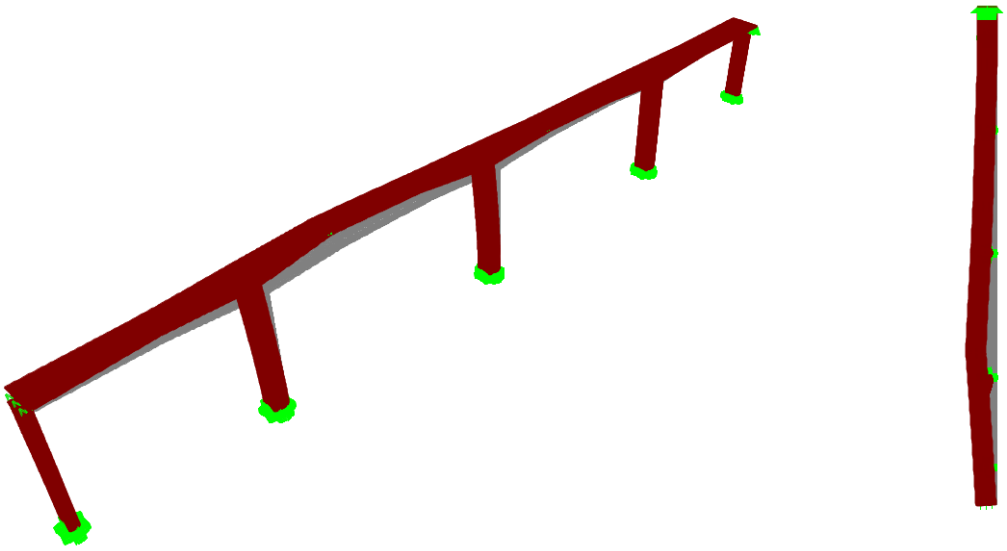

Figure 19: 1st Eigenmode (f=0.617 Hz) translational out-of-plane

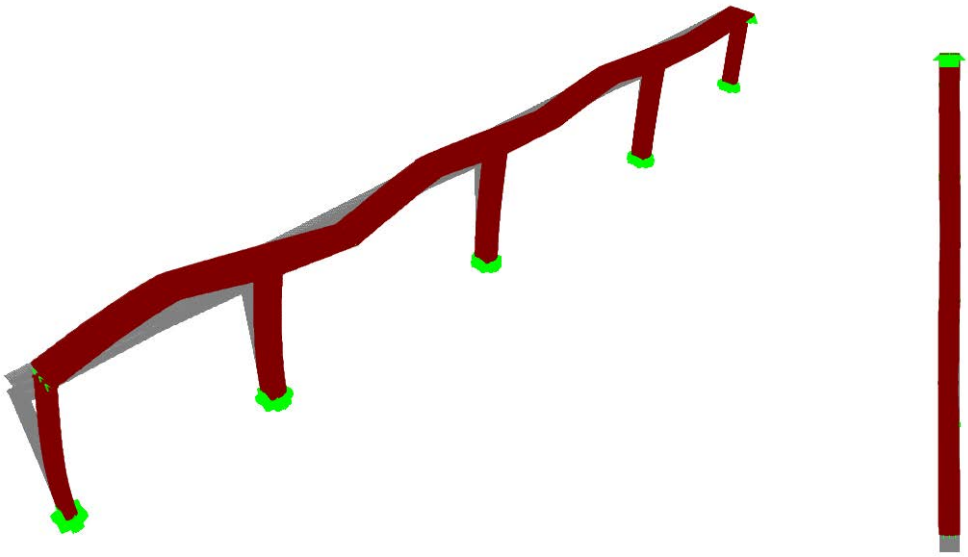

Figure 20: 3rd Eigenmode (f=0.693 Hz) within-plane translational

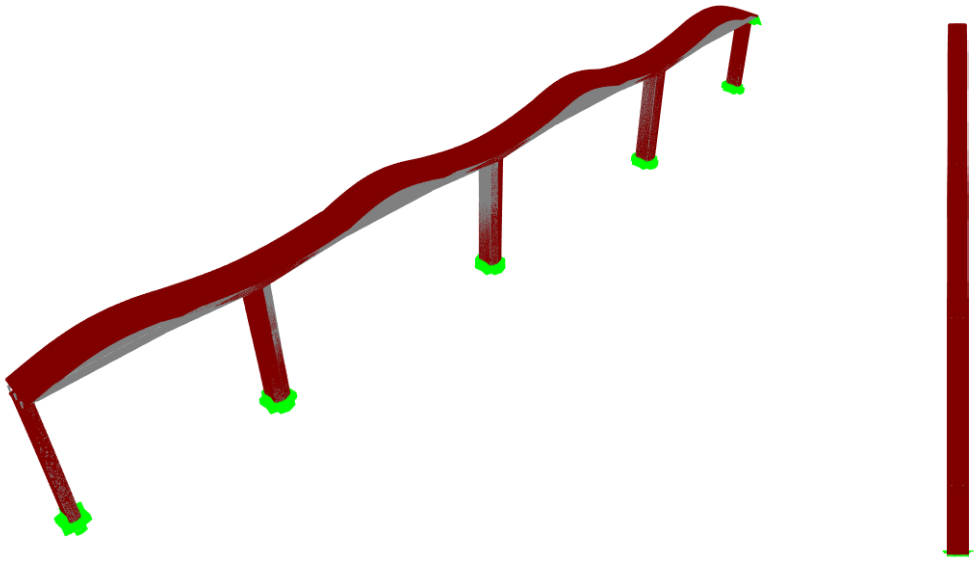

Figure 21: 10th Eigenmode (f=1.753 Hz) translational along the vertical axis

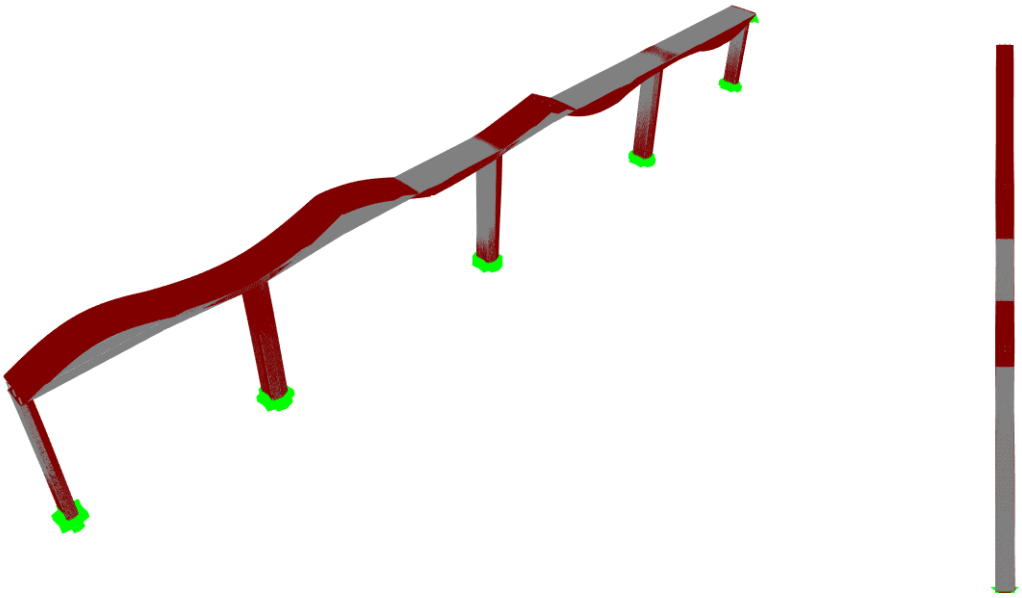

Figure 22: 12th Eigenmode (f=2.074 Hz) in-plane bending

The table below depicts the eigenfrequencies for each of three cases of elastic modulus that came up from shell elements model.

Mode	E=17GPa Frequency(Hz)	E=30GPa Frequency(Hz)	E=34GPa Frequency(Hz)
1	0.476	0.580	0.617
2	0.515	0.617	0.655
3	0.590	0.663	0.693
4	0.623	0.744	0.788
5	0.681	0.834	0.887
6	0.713	0.845	0.891
7	0.924	1.129	1.199
8	1.138	1.380	1.419
9	1.319	1.385	1.472
10	1.373	1.648	1.753
11	1.600	1.833	1.859
12	1.621	1.950	2.074
13	1.829	1.982	2.105
14	1.966	2.347	2.496
15	2.172	2.668	2.836

Table 3: Eigenfrequencies that came from modal analysis of shell elements model.

4.3 Solid elements model

Also, a more sophisticated finite elements model was generated. This includes the one pier only. After modal analysis was done two vertical eigenfrequencies were found. For the case that young modulus was 34 GPa the eigenfrequencies are very close to the measured values. Below depicts the two vertical eigenmodes.

Figure 23: 1th Eigenmode (f=1.435 Hz) translational along the vertical axis

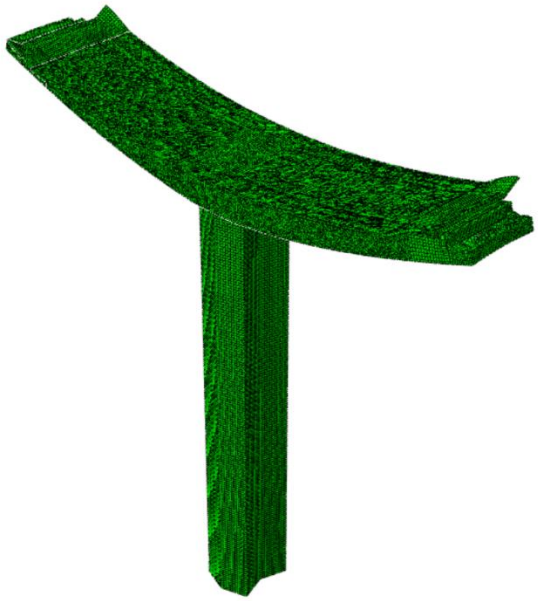

Figure 24: 2th Eigenmode (f=2.16 Hz) in-plane bending

Mode	E=17GPa	E=30GPa	E=34GPa
	Fre-quency(Hz)	Fre-quency(Hz)	Fre-quency(Hz)
1	1.02	1.35	1.435
2	1.537	2.03	2.16

Table 4: Eigenfrequencies in vertical direction that came from modal analysis of solid elements model.

4.4 Discussion

- Between the computational model of cell elements and solid elements there seems to be a greater stiffness in the model of cell elements due to the effect of the Gerber beam.
- Between the in situ measurements there is a differentiation that may be attributable to factors such as the discontinuities of the concrete as well as to the fatigue of the seismic bearings.
- The parametrization of the concrete modulus of elasticity parameter helps us to identify the condition of the existing structure. Indeed, the eigenfrequencies of all three piers are more closely aligned when the Young's modulus is 34GPa.
- In order to improve the accuracy of the analysis and to derive more precise results, it would be desirable to choose a more accurate method of selecting the eigenfrequencies from the in-situ measurements.
- Finally, it would be advisable to compare the eigenfrequencies in the other planes as well.

5 CONCLUSIONS

In this manuscript a further application of structural health monitoring as well as operational modal analysis is presented. This is done on the Servia High Bridge. Shm is a relatively simple method that enables one to easily determine the condition of the structure. It has a broad

significance in civil engineering, especially in civil engineering structures, in particular in bridges, because with the methodology described above one can easily assess the condition of a bridge.

The identification of the eigenfrequencies from in situ accelerometer data after an agitation is a complex procedure as there are several uncertainties in measurement such as weather conditions or external stimuli, which are described in this manuscript. In this manuscript the eigenmodes were selected by the peak-picking method. The selection of these could have been done by a more complex and accurate method in order to avoid any errors related to the presence of other external frequencies. The greater the complexity of the structure, the easier it is for one to be led to erroneous results when determining the eigenfrequencies. The vertically recorded eigenfrequencies were verified against those that emerged from the numerical simulations. Both simulations generated are highly accurate both in terms of the geometrical shape of the bridge and the position of the structure mass. However, they do not take into consideration the realistic interaction between the structure and the soil. It is emphasised however that the eigenmodes could have been authenticated by implementing a simpler beam elements model.

REFERENCES

[1] Neves, A. C., Leander, J., González, I., & Karoumi, R. (2019). An approach to decision-making analysis for implementation of structural health monitoring in bridges. *Structural Control and Health Monitoring*, *26*(6), e2352. **https://doi.org/10.1002/stc.2352**

[2] J.M.W. Brownjohn, Filipe Magalhaes, Elsa Caetano, Alvaro Cunha,Ambient vibration re-testing and operational modal analysis of the Humber Bridge,Engineering Structures,Volume 32, Issue 8,2010,Pages 2003-2018,ISSN 0141-0296,https://doi.org/10.1016/j.engstruct.2010.02.034.

[3] Le Diourion, T., and G. Hovhanessian. "The health monitoring of Rion Antirion Bridge." *IMACXXIII, Orlando* (2005).

[4] Cheung, Mo Shing, et al. "Field monitoring and research on performance of the Confederation Bridge." *Canadian Journal of Civil Engineering* 24.6 (1997): 951.

[5] Wong, K. Y. (2004). Instrumentation and health monitoring of cable-supported bridges. *Structural control and health monitoring*, *11*(2), 91-124.

[6] Frýba, L., & Pirner, M. (2001). Load tests and modal analysis of bridges. *Engineering Structures*, *23*(1), 102-109.

[7] Döhler, M., Hille, F., Mevel, L., & Rücker, W. (2014). Structural health monitoring with statistical methods during progressive damage test of S101 Bridge. *Engineering Structures*, *69*, 183-193.

[8] Reynders, E., Maes, K., Lombaert, G., & De Roeck, G. (2016). Uncertainty quantification in operational modal analysis with stochastic subspace identification: Validation and applications. *Mechanical Systems and Signal Processing*, *66*, 13-30.

[9] Neves, A. C., Gonzalez, I., Leander, J., & Karoumi, R. (2017). Structural health monitoring of bridges: a model-free ANN-based approach to damage detection. *Journal of Civil Structural Health Monitoring*, *7*, 689-702.

[10] Zinno, R., Haghshenas, S. S., Guido, G., Rashvand, K., Vitale, A., & Sarhadi, A. (2022). The State of the Art of Artificial Intelligence Approaches and New Technologies in Structural Health Monitoring of Bridges. *Applied Sciences*, *13*(1), 97.

[11]) Hansen, J. B., Brincker, R., López-Aenlle, M., Overgaard, C. F., & Kloborg, K. (2017). A new scenario-based approach to damage detection using operational modal parameter estimates. *Mechanical systems and signal processing*, *94*, 359-373.

[12] Rosales, M. B., Filipich, C. P., & Buezas, F. S. (2009). Crack detection in beam-like structures. *Engineering Structures*, *31*(10), 2257-2264.

[13] Rainieri, C., & Fabbrocino, G. (2015). Development and validation of an automated operational modal analysis algorithm for vibration-based monitoring and tensile load estimation. *Mechanical Systems and Signal Processing*, *60*, 512-534.

[14] Mousavi, M., & Gandomi, A. H. (2021). Structural health monitoring under environmental and operational variations using MCD prediction error. *Journal of Sound and Vibration*, *512*, 116370.

[15] Peeters, B., & Ventura, C. E. (2003). Comparative study of modal analysis techniques for bridge dynamic characteristics. *Mechanical Systems and Signal Processing*, *17*(5), 965-988.

[16] Reynders, E., & De Roeck, G. (2008). Reference-based combined deterministic–stochastic subspace identification for experimental and operational modal analysis. *Mechanical Systems and Signal Processing*, *22*(3), 617-637.

[17] Magalhães, F., & Cunha, Á. (2011). Explaining operational modal analysis with data from an arch bridge. *Mechanical systems and signal processing*, *25*(5), 1431-1450.

[18] Qu, C. X., Yi, T. H., Li, H. N., & Chen, B. (2018). Closely spaced modes identification through modified frequency domain decomposition. *Measurement*, *128*, 388-392.

[19] Langone, R., Reynders, E., Mehrkanoon, S., & Suykens, J. A. (2017). Automated structural health monitoring based on adaptive kernel spectral clustering. *Mechanical Systems and Signal Processing*, *90*, 64-78.

[20] Yang, Y. B., & Chang, K. C. (2009). Extracting the bridge frequencies indirectly from a passing vehicle: Parametric study. *Engineering Structures*, *31*(10), 2448-2459.

[21] Malekjafarian, A., & OBrien, E. J. (2017). On the use of a passing vehicle for the estimation of bridge mode shapes. *Journal of Sound and Vibration*, *397*, 77-91.

[22] Yang, Y. B., Xu, H., Wang, Z. L., Shi, K., & Wu, Y. T. (2022). Refined detection technique for bridge frequencies using rocking motion of single-axle moving vehicle. *Mechanical Systems and Signal Processing*, *162*, 107992.

[23] Yin, X., Fang, Z., Cai, C. S., & Deng, L. (2010). Non-stationary random vibration of bridges under vehicles with variable speed. *Engineering Structures*, *32*(8), 2166-2174.

[24] Parker Hannifin Corp. (2020). "MicroStrain Sensing Product Datasheet: G-Link_200", Williston, VT, USA: Parker Hannifin Corp.

[25] Parker Hannifin Corp. (2020). "MicroStrain Sensing Product Datasheet: WSDA-2000", Williston, VT, USA: Parker Hannifin Corp.

[26] Brincker, R. and Ventura, C. (2015). "Introduction to operational modal analysis". WestSussex, UK: JohnWiley& Sons, Ltd.

[27] Cooley, J.W. and Tukey, J.W. (1965). “An algorithm for the machine calculation of complex Fourier series”. Mathematics of Computation, 19 (90): 297-301.